Volume 14
Number 16
28 April 2023
Pages 4195–4436

Chemical Science

rsc.li/chemical-science

ISSN 2041-6539

ROYAL SOCIETY OF CHEMISTRY

EDGE ARTICLE

John McCracken, Selvan Demir, Aaron L. Odom *et al.*
A rare isocyanide derived from an unprecedented neutral yttrium(II) bis(amide) complex

Chemical Science

ROYAL SOCIETY OF CHEMISTRY

EDGE ARTICLE

View Article Online
View Journal | View Issue

Cite this: *Chem. Sci.*, 2023, **14**, 4257

All publication charges for this article have been paid for by the Royal Society of Chemistry

Received 10th January 2023
Accepted 11th March 2023

DOI: 10.1039/d3sc00171g

rsc.li/chemical-science

A rare isocyanide derived from an unprecedented neutral yttrium(II) bis(amide) complex†

Rashmi Jena, Florian Benner, Francis Delano, IV, Daniel Holmes, John McCracken, * Selvan Demir * and Aaron L. Odom *

A room temperature stable complex formulated as $Y(NHAr^*)_2$ has been prepared, where Ar* = 2,6-(2,4,6-$(^iPr)_3C_6H_2)C_6H_3$, by KC_8 reduction of $ClY(NHAr^*)_2$. Based on EPR evidence, $Y(NHAr^*)_2$ is an example of a d^1 Y(II) complex with significant delocalization of the unpaired electron density from the metal to the ligand. The isolation of molecular divalent metal complexes is challenging for rare earth elements such as yttrium. In fact, stabilization of the divalent state requires judicious ligand design that allows the metal center to be coordinatively saturated. Divalent rare earth elements tend to be reactive towards various substrates. Interestingly, $Y(NHAr^*)_2$ reacts as a radical donor towards ^{t}BuNC to generate an unusual yttrium isocyanide complex, $CNY(NHAr^*)_2$, based on spectroscopic evidence and single-crystal X-ray diffraction data.

Introduction

Stabilization of metal centers in unusual oxidation states provides opportunities to examine new electronic structures, metal–ligand interactions, and reactivity. While the vast majority of Group 3 transition metals and lanthanide compounds have the metal center in the +3 formal oxidation state, the oxidation states of many of the rare earth metals have been expanded to include examples where the formal oxidation state is +2, and Evans wrote in 2016 that, "Ln^{2+} ions are now known for all the lanthanides except {radioactive} *Pm*."[1]

The first Y(II) complex, $\{Y(C_5H_4SiMe_3)_3\}^-$, was prepared by reduction of the neutral Y(III) complex (Chart 1), and the stability of these complexes is closely tied to the counterion used.[2–4] Recently, an Y(II) complex using tris(aryloxide)mesitylene ligands was reported by Meyer and Evans that is stable for ~48 h at room temperature in THF.[5,6] In addition to cyclopentadienyl and alkoxide ligands, hexamethyldisilazides have been employed.[7,8] In all cases, the currently known yttrium(II) complexes possess very bulky and strongly donating ligands in an approximately trigonal environment around the metal center, and all the ligands are retained on reduction to the anion.

The first fully characterized example of a rare earth η^6-arene complex is $Sm(\eta^6\text{-}C_6Me_6)(\mu^2\text{-}AlCl_4)_3$, reported by Cotton and Schwotzer in 1986.[9] Cloke and coworkers prepared a host of interesting rare earth arene complexes in the apparent zero oxidation state.[10] It is clear from these results that arenes are adept at stabilizing metals in low oxidation states. We wondered if an yttrium bis(η^6-arene) complex in the formal oxidation state of Y(II) could be prepared using this arene coordination strategy to stabilize the low oxidation state. Here, we describe the

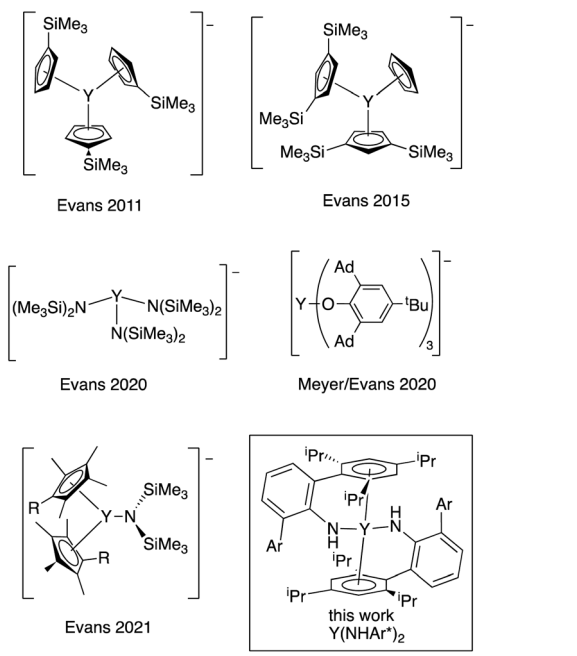

Chart 1 Known Y(II) complexes[2–7] and the complex described here (boxed). Ad = 1-adamantyl. Ar = 2,4,6-$(^iPr)_3C_6H_2$.

Michigan State University, Department of Chemistry, 578 S. Shaw Ln, East Lansing, MI, USA, 48824. E-mail: odoma@msu.edu; sdemir@chemistry.msu.edu; mccracke@msu.edu

† Electronic supplementary information (ESI) available: Detailed synthetic procedures and additional characterization data. X-ray crystallographic data has been deposited. CCDC 2207616–2207618. For ESI and crystallographic data in CIF or other electronic format see DOI: https://doi.org/10.1039/d3sc00171g

synthesis and properties of a neutral Y(II) bis(amide) complex related to a recently reported U(II) system, U(NHAr*)$_2$, where Ar* = 2,6-(2,4,6-^{i}Pr$_3$C$_6$H$_2$)C$_6$H$_3$.[11] In this uranium complex, there is evidence that reduction leads to increased bonding between the metal and the arene groups of the amide, stabilizing the neutral reduced complex. As a result, these ligands seem particularly well suited for the stabilization of highly reducing metal centers like yttrium(II), and Y(NHAr*)$_2$ is relatively stable in diethyl ether at room temperature under inert atmosphere for days.

Based on EPR spectroscopy, the complex is formulated as d^1 Y(II) with a significant portion of the unpaired electron density residing on the metal center. Despite possessing good thermal stability, the yttrium(II) complex is quite reactive, which we demonstrate through the synthesis and characterization of a new *isocyanide* CN–Y(NHAr*)$_2$, where the CN ligand is only bound through nitrogen. The complex is prepared by presumed radical cleavage of a C–C or C–N bond. Evidence for this binding mode and discussion of when such a mode might be more favorable than the more common C-bound cyanide are included.

Results and discussion

Synthesis and properties of Y(NHAr*)$_2$

Unsolvated KNHAr* was prepared in 64% yield by addition of solid KCH$_2$SiMe$_3$ to H$_2$NAr* in *n*-hexane.[11–13] Salt metathesis of YCl$_3$ in diethyl ether with 2 equiv. of KNHAr* resulted in the formation of ClY(NHAr*)$_2$ (**1**) (Fig. 1). Single-crystal X-ray diffraction on **1** revealed an η^6-interaction (Ar1 in Fig. 1, red) between one of the arene substituents of an NHAr* ligand and yttrium. The η^6-arene centroid to Y distance was found to be 2.493(3) Å, whereas the next closest Y-(arene centroid) distance is 3.699(3) Å. However, ^{1}H and ^{13}C NMR spectroscopy suggests all the arene rings are equivalent on the timescale of these experiments, indicating that fast exchange occurs between the bound and unbound aromatic groups of **1** in solution.

The centroid-(Ar1)–Y1–N1 angle is 94.9(7)°, and the centroid (Ar1)–Y1–N2 angle is 101.8(6)°. The Y1–N1 distance is 2.249(2) Å, and Y1–N2 is 2.210(2) Å for the two inequivalent amides. The Y1–N1–C1(*ipso*) angle is 131.5(2)°, and Y1–N–C36(*ipso*) is 144.0(2)°, with the large disparity caused by the η^6-arene coordination to only one ligand.

Treatment of ClY(NHAr*)$_2$ (**1**) with excess KC$_8$ results in a color change from light yellow to a very dark yellow within an hour (Fig. 2). The product formed, Y(NHAr*)$_2$ (**2**), retains its color as a clear yellow diethyl ether solution at room

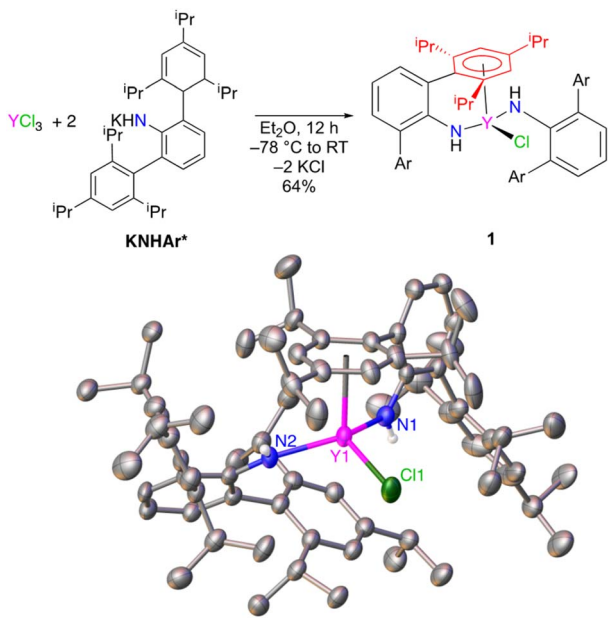

Fig. 1 Synthesis of ClY(NHAr*)$_2$ (**1**) (top) and (bottom) the structure of **1** from single-crystal X-ray diffraction (thermal ellipsoids drawn at 50%), where Ar is 2,4,6-(^{i}Pr)$_3$C$_6$H$_2$. Hydrogen atoms on carbon and solvent molecules (2 *n*-hexane) are not shown for clarity. The η^6-arene (red) is discussed as Ar1 in the text. Some selected structural parameters: Y–N distances: 2.249(2) Å, 2.210(2) Å. Y–Ar1(centroid): 2.493(3) Å.

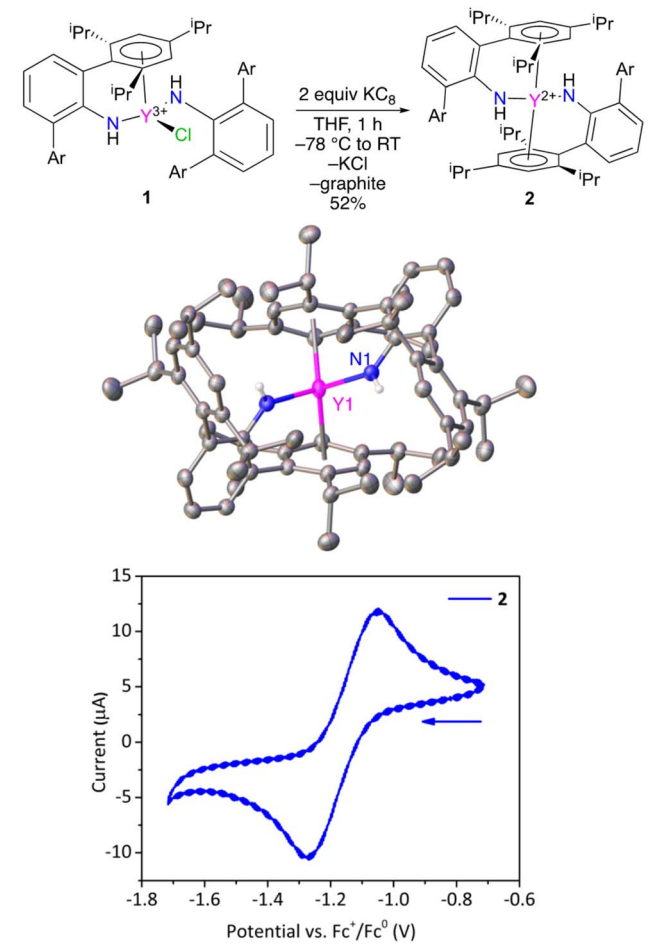

Fig. 2 (top) Synthesis of **2** and (middle) structure of Y(NHAr*)$_2$ from single-crystal X-ray diffraction (thermal ellipsoids drawn at 50%), where Ar is 2,4,6-(^{i}Pr)$_3$C$_6$H$_2$. Hydrogen atoms on carbon and solvent molecule (THF) in the crystal lattice are not shown for clarity. The molecule resides on a crystallographic 2-fold axis. Some selected parameters: Y–N: 2.261(1) Å. Y–Ar(centroid): 2.468(8) Å. (bottom) Cyclic voltammogram of **2** (1.5 mM) in Et$_2$O with 0.1 M NBu$_4^+$ B(3,5-(CF$_3$)$_2$C$_6$H$_3$)$_4^-$ as electrolyte, 100 mV s^{-1} scan rate, with a glassy carbon working electrode.

temperature for at least 1 week. We observed dilute ether solutions at room temperature for >100 h, and decomposition seemed have a rate of ~3% per day under these conditions (see the ESI† for more details.)

X-ray diffraction quality crystals of **2** were obtained from *n*-hexane, and the geometries of **1** and **2** vary significantly in the solid-state. Complex **2** crystallizes on a 2-fold rotation axis bisecting the N–Y–N angle, Fig. 2 and S28.† In this case, *ortho*-aromatic rings from both amide groups are η^6-coordinated to the metal center, similar to previously reported U(NHAr*)$_2$.[11]

In this lower oxidation state, the Y1–Ar1(centroid) distance shortened slightly (but not significantly relative to three times the e.s.d.) relative to **1** from 2.493(3) Å to 2.468(8) Å in **2**. Naturally, the expectation is that the radius of the metal will increase on reduction, which is observed in the Y–N distance in **1** *vs.* **2** of 2.230(2) *vs.* 2.261(1) Å, respectively. The apparent contraction in Y–Ar(centroid) distance in **2** *vs.* **1** is consistent with additional yttrium to arene bonding between the formally reduced metal center to the arene in the reduced complex, an effect observed in the related U(NHAr*)$_2$ complex as well.[11]

Y(II) complex **2** was examined by cyclic voltammetry (Fig. 2) using NBu_4^+ B(3,5-$(CF_3)_2C_6H_3)_4^-$ as the electrolyte in diethyl ether with a glassy carbon working electrode. A reversible feature was observed at $E_{1/2} = -1.16 \pm 0.01$ V in the voltammogram (see the ESI†) *vs.* $FeCp_2^{+1/0}$ under these conditions, which is assigned to the Y(NHAr*)$_2^{+1/0}$ couple (Fig. 2, bottom). For comparison, a recent report listed the quasi-reversible Y$(C_5H_4SiMe_3)_3^{-/0}$ potential as $E_{1/2} = -3.06$ V in THF with NBu_4^+ BPh_4^- as electrolyte.[14] One can readily see the extreme difference in the two metal environments. Complex **2** contains aromatic groups that we believe act as acceptors, making the complex more stable and much more readily reduced, while Y$(C_5H_4SiMe_3)_3$ contains anionic (presumably strongly donating) cyclopentadienyls that make the metal quite difficult to reduce.

EPR spectra collected for Y(NHAr*)$_2$ (**2**) in Et_2O at 60 K and 295 K are shown in Fig. 3. The frozen solution spectrum (top, black trace) shows an axial lineshape with hyperfine splitting that arises from an $I = 1/2$ nucleus, consistent with an ^{89}Y-centered paramagnet. Analysis of this spectrum shows that it can be well-simulated (top, red trace) using an axial *g*-tensor with $g_\parallel = 1.985$ and $g_\perp = 2.004$, an axial ^{89}Y hyperfine coupling with $A_\parallel = 38.9$ MHz and $A_\perp = 40.9$ MHz, and an intrinsic Gaussian lineshape with an average width of 1.06 mT (FWHM). The solution spectrum of **2** in Et_2O (bottom, black trace) features a broad intrinsic lineshape with a modest inflection, also consistent with hyperfine splitting from an $I = 1/2$ nucleus. This spectrum was simulated using both fast- and slow-motion calculation models (bottom, red trace). The results of both approaches yield isotropic *g*- and ^{89}Y-hyperfine coupling values of 1.995 and 49 MHz, respectively.[15] For these simulations, a broad Lorentzian intrinsic lineshape of 2.5 mT was required, casting greater uncertainty on the spin Hamiltonian values obtained from the solution spectrum.

The spin Hamiltonian values obtained from analysis of the solid state spectrum of **2** are most similar to those reported for the Y$(C_5H_4SiMe_3)_3^-$ complexes reported by Evans and coworkers.[4] These complexes also showed a modest *g*-anisotropy, $g_\parallel = 2.00$ and $g_\perp = 1.99$, but with $g_\parallel > g_\perp$. For **2**, our analysis shows $g_\parallel < g_\perp$, most likely reflecting the different coordination geometry of the ligands about the metal center.[16] For both **2** and Y$(C_5H_4SiMe_3)_3^-$, the presence of at least one *g*-value below 2.0023 and a resolved $I = 1/2$ isotropic hyperfine coupling is indicative of a d^1-centered paramagnet. The isotropic hyperfine coupling attributed to ^{89}Y of **2** (40.2 MHz) is 40% of that reported for Y$(C_5H_4SiMe_3)_3^-$, consistent with more of the unpaired spin being delocalized onto the NHAr* ligands. This picture of **2**'s electronic structure is supported by the lack of detectable ^{14}N hyperfine coupling in both liquid and solid state EPR spectra. Still, it is worth noting that in single crystal EPR studies of Y(II) in $SrCl_2$, ^{89}Y isotropic hyperfine couplings of 80.8 MHz were resolved.[17] DFT calculations on **2** are consistent with this EPR analysis, showing extensive unpaired spin on the metal and coordinated rings with little on the nitrogen atoms (see the ESI† for more details).

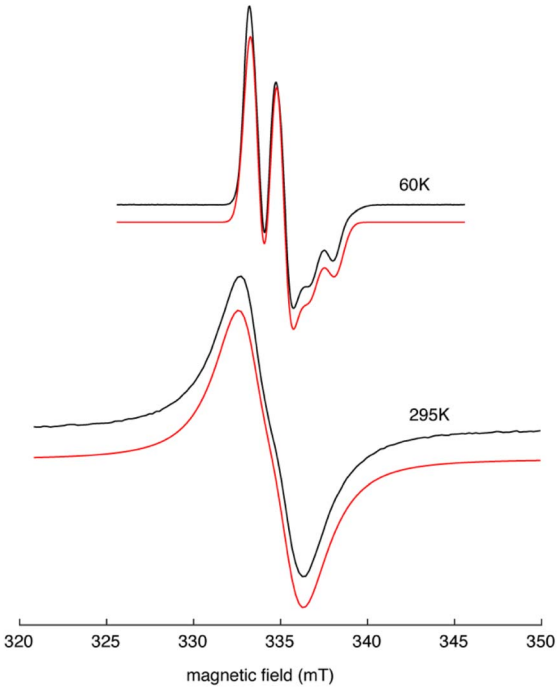

Fig. 3 EPR spectra of Y(NHAr*)$_2$ (**2**) in Et_2O at 60 K (top) and 295 K (bottom). The black traces are the experimental spectra collected using the following conditions: microwave frequency, 9.3972 GHz (top), 9.3270 GHz (bottom); microwave power, 5 mW (top), 0.125 mW (bottom); field modulation amplitude, 0.1 mT (top), 0.4 mT (bottom). The red traces are spectra simulations offset for visualization purposes. Simulations were done with EasySpin[15] using the spin Hamiltonian parameters given in the text.

The compound was examined in the solid-state using SQUID magnetometry (Fig. 4 and additional information in the ESI†). The fits of the $\chi_M T$ *vs.* *T* data engendered slightly lower *g* values than the expected *g* value of 2.0023 for an unpaired electron that is unaffected by spin–orbit coupling. Hence, the isothermal field-dependent magnetization (*M* *vs.* *H*) data were collected between 2 and 10 K up and at fields up to 7 T. The resulting experimental data was fit to a set of Brillouin functions to afford

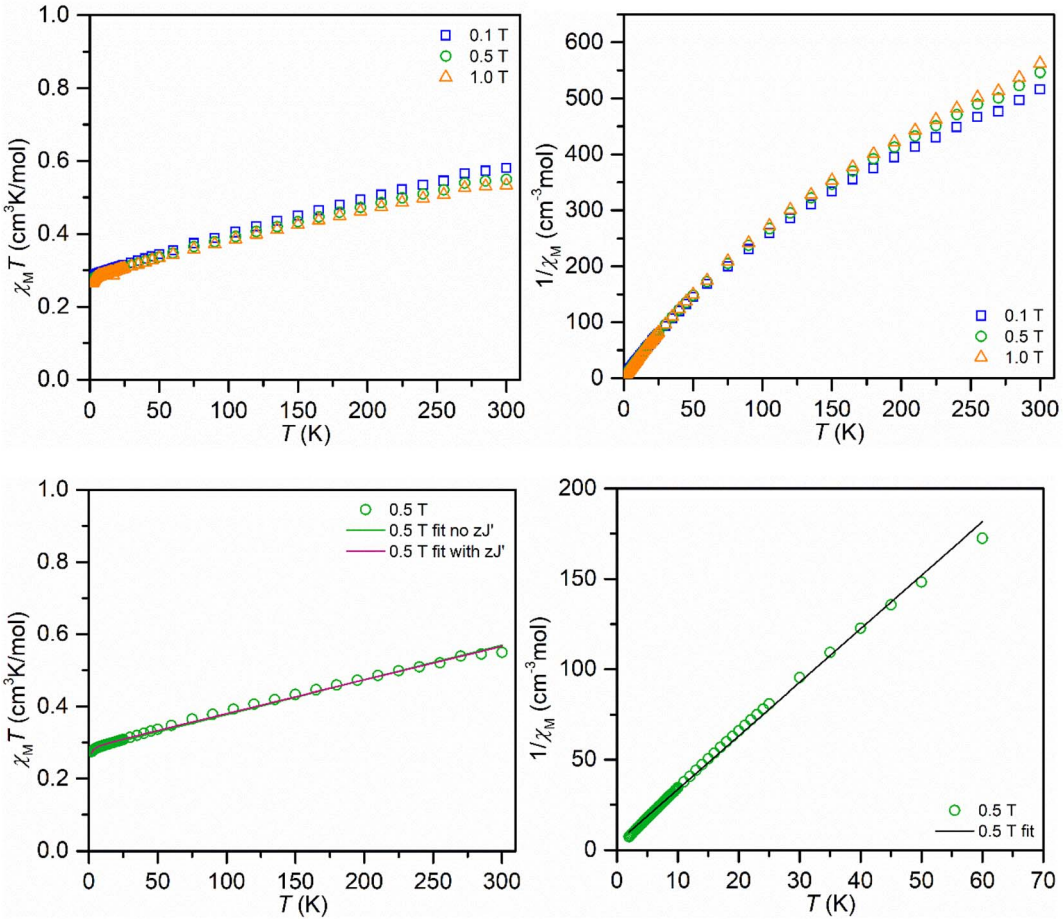

Fig. 4 Variable-temperature dc magnetic susceptibility data for a restrained polycrystalline sample of Y(NHAr*)$_2$ (**2**) collected under 0.1 T, 0.5 T and 1.0 T applied dc fields and at temperatures from 2 to 300 K (top left). Corresponding Curie–Weiss plots ($1/\chi_M$ *vs. T*) for **2** at 0.1 T, 0.5 T and 1.0 T (top right). Explementary fits for $\chi_M T$ *vs. T* (bottom left) and $1/\chi_M$ *vs. T* plots at 0.5 T. Parameters for the χ_M *vs. T* fit: $g = 1.7334(14)$, TIP $= 9.586(51) \times 10^{-4}$ and $g = 1.7521(19)$, TIP $= 9.297(45) \times 10^{-4}$, $zJ' = -0.1195(102)$ cm^{-1}. Parameters for the $1/\chi_M$ *vs. T* fit: $C = 0.338(22)$ cm^3 K mol^{-1}, $\Theta = -1.298$ K.

g values near the expected value (1.9938(19)–2.3163(36)), which are in excellent agreement with the values attained from EPR spectroscopy. The magnetic properties of **2** were also probed through measuring a toluene solution of **2** employing Evans's method between temperatures of 183 and 298 K, Fig. S17.† Similar to the determined $\chi_M T$ values on the solid sample, a higher magnetic moment $\mu_{eff} = 2.39\mu_B$ was obtained relative to the spin-only value of $1.73\mu_B$ for an unpaired electron, which is likely ascribed to a TIP contribution.

The absorption spectrum of **2** in the UV-Vis-NIR was obtained in diethyl ether. The yellow–brown complex has large, intense bands at 752 nm ($\varepsilon = 605$ cm^{-1} M^{-1}), 244 nm ($\varepsilon = 7300$ cm^{-1} M^{-1}), and 297 nm ($\varepsilon = 1040$ cm^{-1} M^{-1}), all assigned to charge transfer transitions. Similar absorptions occur in the previously reported U(II)(NHAr*)$_2$ (ref. 11) (see the ESI† for more details.)

An yttrium isocyanide: CN–Y(NHAr*)$_2$

The reactivity of Y(NHAr*)$_2$ (**2**) was explored as well. The compound is expected to be a high energy metallaradical, and it was anticipated that the complex would react with CN^{t}Bu to liberate (presumably) a *tert*-butyl radical. This was found to be the case; however, instead of producing the more common cyanide (M–CN) the *isocyanide* (M–NC) complex is isolated (Fig. 5).[18,19] The same reaction with NC^{t}Bu provided the same product by ^{1}H NMR spectroscopy.

Within the rich chemistry of isonitrile (CNR) reactions with metal complexes,[20] there are a few other instances where nitriles and isonitriles have been used to add a CN (cyanide or isocyanide) ligand to a metal center. Carmona, Andersen, and coworkers showed that tris(cyclopentadienyl)uranium(III) complexes will react with CN^{t}Bu to give cyanide uranium(IV).[21] Jones and coworkers have extensively studied the isonitrile (and related nitrile) cleavage reactions with nickel(0), ruthenium(0), and iron(0).[22–27] Co(I),[28,29] Sm(II),[30,31] and V(II)[32] complexes have exhibited such reactions, as well. Maron, Arnold, and coworkers used the same reaction to add a CN ligand to a low oxidation state thorium complex.[33]

A couple of different avenues were readily available to determine experimentally that **3** is indeed an isocyanide. The

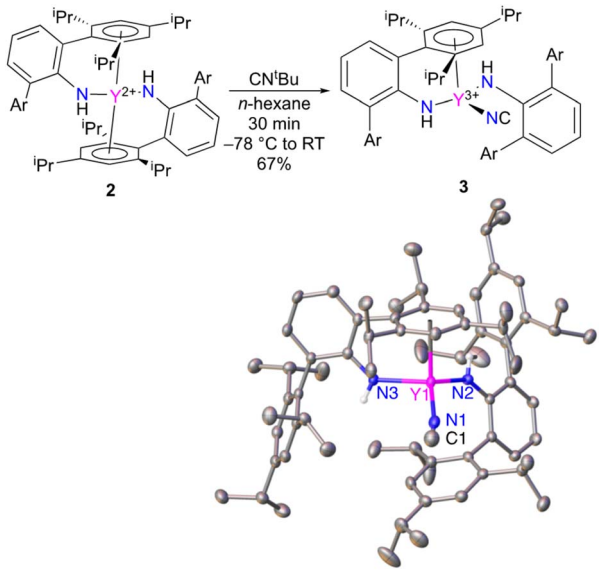

Fig. 5 Synthesis of CN–Y(NHAr*)$_2$ (**3**) (top) and structure from single crystal X-ray diffraction (thermal ellipsoids at 50%), where Ar is 2,4,6-(^{i}Pr)$_3$C$_6$H$_2$. (bottom) Hydrogen atoms on the carbon atoms and solvent molecules in the crystal lattice are not shown for clarity. Selected bond distances (Å) and angles (°): Y1–N1: 2.348(2), Y1–N2: 2.221(2), Y1–N3: 2.221(2), C1–N1: 1.039(4), Y1–N1–C1: 170.4(2)°.

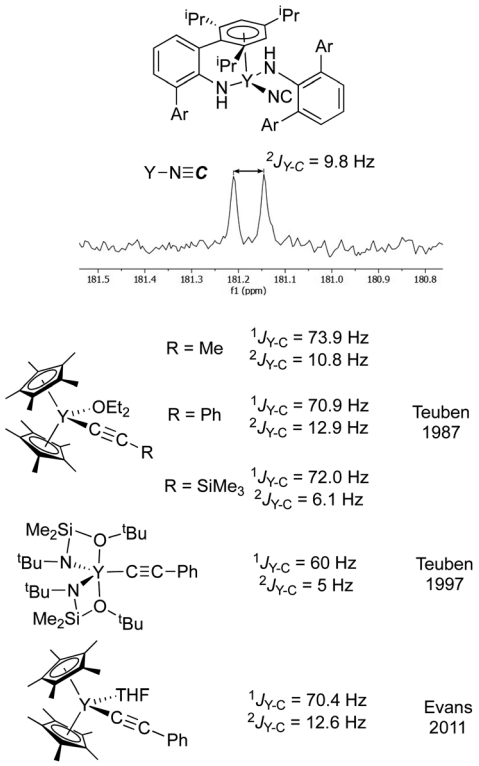

Fig. 6 (top) Excerpt of the ^{13}C NMR spectrum for **3** showing the isocyanide resonance coupled to yttrium. (bottom) The isocyanide resonance is compared with Y–C one- and two-bond coupling constants for some representative alkynyl complexes from Teuben and Evans.[34,36,37] The coupling constant observed for **3** is in the typical range for a two-bond coupling, much smaller than a typical one-bond coupling constant. Ar = 2,4,6-(^{i}Pr)$_3$C$_6$H$_2$.

first is to examine the X-ray diffraction data (Fig. 5) modelled as both the isocyanide and cyanide to see which configuration gives better statistics for the structure. The assigned isocyanide Y–NC structure has R_1 = 4.11% and wR_2 = 9.53%, while the cyanide has R_1 = 4.37% and wR_2 = 10.61%. In addition, the isocyanide structure has improved thermal parameters over the cyanide isomer. More details can be found in the ESI.†

As a second method of determining the relative position of the carbon in the CN ligand, we turned to NMR spectroscopy. First, we were able to account for every observable proton and carbon in the ^{1}H and ^{13}C spectra, which was consistent with the structure shown in Fig. 5. There were no observable couplings between the protons and the carbon assigned to the CN ligand, which argues against a "Y–NCH" structure. The ^{89}Y–^{13}C coupling constant was found to be 9.8 Hz in the ^{13}C NMR spectrum (Fig. 6). Perhaps the best method for relating this to cyanide *vs.* isocyanide couplings is to look at the ^{89}Y–^{13}C coupling constants for the α- and β-carbon atoms of alkynyls, and a few examples are shown in Fig. 6.[34–40] The typical range for the one-bond coupling constant to the α-carbon atom of an alkynyl is 50–75 Hz. While the two-bond couplings to the β-carbon atom of an alkynyl are typically 5–15 Hz. As a result, **3** falls in the middle of the two-bond coupling range, consistent with an isocyanide and is quite distinct from the typical one-bond coupling.

Yttrium features 100% abundance of an NMR active nucleus, ^{89}Y with I = 1/2, and ^{89}Y NMR chemical shifts can be obtained for **1** and **3**. Experimental determination of the chemical shift of **2** was inhibited, as would be expected, by the paramagnetic nature of the Y(III) ion. The ^{89}Y NMR spectra were recorded in toluene-d_8 solutions for **1** and **3** (Fig. S3, S8 and S9†). While ClY(NHAr*)$_2$ (**1**) has a chemical shift for the metal center at +427.7 ppm, the resonance in CN–Y(NHAr*)$_2$ (**3**) is observed at +350.0 ppm. For comparison, the ^{89}Y NMR chemical shifts for the metal centers in Y{N(SiMe$_3$)$_2$}$_3$ and Y(C$_5$H$_4$Me)$_3$(THF) were found at +570 (CDCl$_3$) and −371 ppm (THF), respectively.[41,42]

As an addition to the experimental investigations, we examined the cyanide and isocyanide computationally using DFT. It was found that the N-bound isocyanide is indeed ~4 kcal mol^{-1} lower in energy than the cyanide for this Y(III) system (see ESI† for more details.)

While rare, isocyanides are known, especially for the main group and f-block elements. For example, there is the well-characterized Mg(dipyrrolylmethene)isocyanide reported by Harder and coworkers in 2019,[43] and a report of a thallium porphyrin complex.[44] In the f-block, thorium and uranium isocyanide complexes have been well-established.[33,45–49] One obvious conclusion from the extensive work of Ephritikhine and coworkers on uranium CN complexes is that small changes in structure can change a cyanide ligand into an isocyanide.[47] Indeed calculations on a large number of cyanide *vs.* isocyanide energies suggest that increased covalency favors the cyanide M–CN conformation and ionic structures can slightly favor the isocyanide M–NC structure (*vide infra*).[43] Well-characterized examples of isocyanides of the transition metals seem rarer

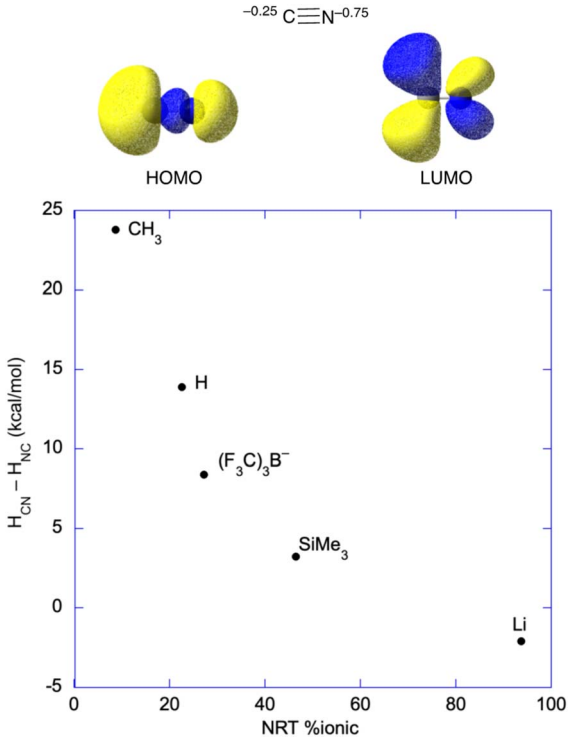

Fig. 7 (top) Natural population analysis gives the anion charge which is 75% on the nitrogen atom, and MO analysis gives that both the HOMO and the LUMO are centered on the carbon. In covalent systems and/or systems with significant backbonding, binding through the carbon is expected based on the MOs; however, very polar systems may bind to the nitrogen of cyanide. (bottom) Plot of the enthalpy difference[57–61] between the cyanide (*e.g.*, HCN) and isocyanide (*e.g.*, HNC) structures *vs.* the percentage of ionic bonding from Natural Resonance Theory (NRT).[62]

than of the f-block metals and main group. Structurally characterized, terminal cyanides of Group-3 elements seem to be quite rare in general.

The IR spectrum for **3** shows an intense band at 2053 cm^{-1} in *n*-hexane at room temperature assigned to the isocyanide stretch. The CN-triple bond stretches in the CN^tBu and NC^tBu starting materials appears at 2125 and 2250 cm^{-1}, respectively. The cyanide stretch in NBu_4^+ CN^- is found at 2050 cm^{-1}.[47] The isocyanide stretch here is quite similar to other reported metal isocyanides such as Arnold and coworkers' thorium complex (2046 cm^{-1}),[33] along with Ephritikhine and coworkers' CN–U $\{N(SiMe_3)_2\}_3$ (2044 cm^{-1}) and NEt_4^+ $(CN)_2U\{N(SiMe_3)_2\}_3^-$ (2058 cm^{-1}).[47] In Harder's magnesium complex, both cyanide and isocyanide are observable in equilibrium with stretching frequencies of 2162 and 2085 cm^{-1}, respectively.[43]

The ~100 cm^{-1} difference in stretching frequency when a substituent is bound to the carbon *vs.* nitrogen atom of the CN triple bond fragment is likely due to the expected difference in alleviating lone pair bond weakening on those atoms.[50] In CN^-, both atoms contain a lone pair of electrons. A lone pair will require more s-character than the only other orbital using s-character in the ligand—the C–N σ-bond (Bent's Rule).[51,52] However, the more electronegative nitrogen atom will be able to support the lone pair of electrons with less s-character than the carbon atom. All of this is borne out by Natural Bond Orbital calculations on the cyanide anion (M06L, def2-tzvp, NBO7), which gives that the nitrogen and carbon lone pairs are held by $sp^{1.1}$- and $sp^{0.55}$-hybrids, respectively. The C–N σ-bond is calculated by NBO to be comprised of overlapping carbon-based $sp^{1.5}$- and nitrogen-based $sp^{0.9}$ orbitals. When another atom binds to the lone pair, some or all the lone pair bond weakening is alleviated, and more s-character can be used in the C–N σ-bond, often strengthening the bond.

There is very little difference in hybridization between the lone pair and σ-bonding orbital on the nitrogen atom ($sp^{0.9}$ *vs.* $sp^{1.1}$), while there is a larger difference for the carbon atom ($sp^{1.5}$ *vs.* $sp^{0.55}$). Consequently, very little additional C–N bonding is gained by the metal bonding to the nitrogen atom, and the CN stretching frequency does not change a great deal from free CN^- for isocyanide systems (assuming no significant backbonding). In contrast, the CN bond can strengthen more significantly when a non-backbonding metal is attached to the carbon atom, and the stretching frequency *increases* over free cyanide anion. This effect to increase the bond strength and stretching frequency, which occurs in CO chemistry as well, is sometimes referred to as "nonclassical" bonding for the ligand since the CO (or CN^-) increases in stretching frequency and bond strength instead of weakening, as would be expected in systems where backbonding to the diatomic occurs.[53–56] As a result, the slightly lower frequency of the isocyanide stretch relative to related cyanide complexes is not likely to be due to increased backbonding but is instead due to differences in lone pair bond weakening in the two bonding modes of the ambidentate ligand.

Conclusions

Using a triarylamide ligand (NHAr*), we were able to prepare a thermally stable Y(II) complex, $Y(NHAr^*)_2$ (**2**). The compound exhibits a geometry similar to previously reported $U(NHAr^*)_2$ with an aryl ring of each amide η^6-bound to the metal center to give a sandwich structure (Fig. 2). The complex was prepared by chemical reduction of $ClY(NHAr^*)_2$ (**1**), a half-sandwich complex, with the strong reductant KC_8, potassium graphite. Cyclic voltammetry on **2** shows a reversible feature at −1.16 ± 0.01 V relative to $FeCp_2^{+/0}$ in Et_2O assigned to the $Y(NHAr^*)_2^{+/0}$ couple. By EPR, the unpaired electron-density in **2** is delocalized with significant yttrium character, and we assign the complex as Y(II) d^1.

The strongly reducing radical **2** is quite reactive despite being relatively stable under inert atmosphere at room temperature in diethyl ether. Reaction of **2** with CN^tBu or NC^tBu results in supposed loss of *tert*-butyl radical and formation of the unusual isocyanide, $CN–Y(NHAr^*)_2$ (**3**), a half-sandwich complex. The isocyanide structure was assigned based on single-crystal X-ray diffraction and the ^{89}Y–^{13}C coupling constant in the ^{13}C spectrum, which is consistent with a two-bond coupling in relation to known yttrium acetylides (Fig. 6). Further, the IR stretching frequency for isocyanide metal complexes are expected to be somewhat lower (~100 cm^{-1}) than

cyanide stretching frequencies (negligible backbonding in all cases), and **3** is similar to other known isocyanide complexes in CN stretching frequency. DFT calculations on CN–Y(NHAr*)$_2$ (**3**) and hypothetical NC–Y(NHAr*)$_2$ suggest the isocyanide is more stable by ~4 kcal mol^{-1}.

As mentioned, well-characterized examples of transition metal isocyanides seem to be quite rare; however, there are well established examples for the main group and f-block elements. Their existence anywhere in the periodic table as stable species is somewhat surprising based on a molecular orbital analysis of the cyanide ion, which has both the HOMO and LUMO predominantly on carbon (Fig. 7), something that is obvious from the orbital pictures (M06/def2-tzvp). However, Natural Population Analysis gives that about 75% of the anionic charge of cyanide resides on nitrogen. Consequently, metal centers that are very electropositive and with little or no ability to backbond to CN$^-$ may favor the isocyanide structure. Put another way, highly polar systems may give the charge-controlled structure (as opposed to frontier orbital controlled structure) with the nitrogen bound to the metal center.[63–66]

The structural effects of a highly polar bond were discussed by Harder and coworkers on their article regarding a Mg–CN complex, where they pointed out that more X–CN (where X–CN = MeCN, HCN, $(F_3C)_3BCN^-$, Me_3SiCN, and LiCN)[57–61] covalency leads to thermodynamically favored carbon-bonding, as opposed to nitrogen in the cyanide unit, and higher barriers to generating the isocyanide.[43] Natural Resonance Theory (NRT) can be used to determine the ionic character in these main group systems, which is plotted against the enthalpic favorability of the ground state cyanide (X–CN) structure in Fig. 7.[62] Clearly, the more covalent systems, *e.g.*, H_3C–CN, favor binding through carbon, while bonding to nitrogen only becomes favorable for very polar systems like LiCN, where H_{CN}–H_{NC} = −2 kcal mol^{-1}.

Currently, we are examining related f-block systems using these intriguing ligands.

Data availability

The ESI† contains all spectroscopy, characterization data, and computational data. Structures are available on CCDC.

Author contributions

RJ prepared all the compounds in the paper and aided with characterization. FB and FD did the initial preparation of **1**. FB and RJ collected and analyzed the CV data. DH was instrumental in NMR characterization of **3**. JM collected and analyzed the EPR spectroscopic data. SD and ALO conceived the project, provided resources, and support. ALO wrote the initial draft of the article, and all authors aided in editing.

Conflicts of interest

There are no conflicts to declare.

Acknowledgements

ALO would like to thank the National Science Foundation (CHE-1953254) and the American Chemical Society Petroleum Research Fund (65702-ND3) for support of their research. S. D. is grateful to the Department of Chemistry at Michigan State University (MSU) for generous start-up funds. We extend our thanks to Prof. James K. McCusker for providing access to the UV-Vis-NIR spectrophotometer and Dr Richard J. Staples for his assistance in the interpretation of the collected X-ray diffraction data. Funding for the single-crystal X-ray diffractometer was provided through the MRI program of the National Science Foundation under Grant No. MRI-1919565.

References

1 W. J. Evans, *Organometallics*, 2016, **35**, 3088–3100.
2 M. R. MacDonald, J. E. Bates, J. W. Ziller, F. Furche and W. J. Evans, *J. Am. Chem. Soc.*, 2013, **135**, 9857–9868.
3 M. R. MacDonald, J. W. Ziller and W. J. Evans, *J. Am. Chem. Soc.*, 2011, **133**, 15914–15917.
4 W. N. G. Moore, J. W. Ziller and W. J. Evans, *Organometallics*, 2021, **40**, 3170–3176.
5 S. A. Moehring, M. Miehlich, C. J. Hoerger, K. Meyer, J. W. Ziller and W. J. Evans, *Inorg. Chem.*, 2020, **59**, 3207–3214.
6 C. T. Palumbo, D. P. Halter, V. K. Voora, G. P. Chen, J. W. Ziller, M. Gembicky, A. L. Rheingold, F. Furche, K. Meyer and W. J. Evans, *Inorg. Chem.*, 2018, **57**, 12876–12884.
7 A. J. J. Ryan, J. W. Ziller and W. J. Evans, *Chem. Sci.*, 2020, **11**, 2006–2014.
8 T. F. Jenkins, S. Bekoe, J. W. Ziller, F. Furche and W. J. Evans, *Organometallics*, 2021, **40**, 3917–3925.
9 F. A. Cotton and W. Schwotzer, *J. Am. Chem. Soc.*, 1986, **108**, 4657–4658.
10 F. G. N. Cloke, *Chem. Soc. Rev.*, 1993, **22**, 17–24.
11 B. S. Billow, B. N. Livesay, C. C. Mokhtarzadeh, J. McCracken, M. P. Shores, J. M. Boncella and A. L. Odom, *J. Am. Chem. Soc.*, 2018, **140**, 17369–17373.
12 B. Twamley, C. S. Hwang, N. J. Hardman and P. P. Power, *J. Organomet. Chem.*, 2000, **609**, 152–160.
13 P. L. Arnold and S. T. Liddle, *C. R. Chim.*, 2008, **11**, 603–611.
14 M. T. Trinh, J. C. Wedal and W. J. Evans, *Dalton Trans.*, 2021, **50**, 14384–14389.
15 S. Stoll and A. Schweiger, *J Mag. Res.*, 2006, **178**, 42–55.
16 J. R. Pilbrow, *Transition Ion Electron Paramagnetic Resonance*, Oxford University Press, 1990.
17 J. R. Herrington, T. L. Estle and L. A. Boatner, *Phys. Rev. B: Solid State*, 1973, **7**, 3003–3013.
18 G. P. Moss, P. A. S. Smith and D. Tavernier, *Pure Appl. Chem.*, 1995, **67**, 1307–1375.
19 In 1995, IUPAC guidelines suggested the use of "cyanide" for salts of CN$^\bullet$ and C-organyl derivatives of hydrogen cyanide, HCN, *e.g.*, CH_3CN as "methyl cyanide" rather than the more common "acetonitrile". It would have been less confusing to call metal-CN complexes "cyanides" and the

organic compounds nitriles, following common usage. In addition, the same recommendations described the term "isonitrile" as "An obsolete term, which should not be used, for isocyanides." In other words, they describe RNC compounds as "isocyanides" and disposed of "isonitrile" as archaic. Unfortunately, these recommendations cause great confusion when trying to describe complexes of the type M–NC. These N-bound cyanides should be rightfully called "isocyanide complexes" but are conflated with RNC–M compounds of the same name, where the latter should have been uniquely named "isonitrile complexes". All this confusion aside, we will use the term that could have been reserved for M–NC species here, "isocyanides".

20 V. P. Boyarskiy, N. A. Bokach, K. V. Luzyanin and V. Y. Kukushkin, *Chem. Rev.*, 2015, **115**, 2698–2779.
21 M. D. Conejo, J. S. Parry, E. Carmona, M. Schultz, J. G. Brennann, S. M. Beshouri, R. A. Andersen, R. D. Rogers, S. Coles and M. Hursthouse, *Chem.–Eur. J.*, 1999, **5**, 3000–3009.
22 M. E. Evans, T. Li and W. D. Jones, *J. Am. Chem. Soc.*, 2010, **132**, 16278–16284.
23 C. L. Tennent and W. D. Jones, *Can. J. Chem.*, 2005, **83**, 626–633.
24 J. J. Garcia, A. Arevalo, N. M. Brunkan and W. D. Jones, *Organometallics*, 2004, **23**, 3997–4002.
25 J. J. Garcia, N. M. Brunkan and W. D. Jones, *J. Am. Chem. Soc.*, 2002, **124**, 9547–9555.
26 J. J. Garcia and W. D. Jones, *Organometallics*, 2000, **19**, 5544–5545.
27 W. D. Jones and W. P. Kosar, *Organometallics*, 1986, **5**, 1823–1829.
28 X. Y. Li, H. J. Sun, F. L. Yu, U. Florke and H. F. Klein, *Organometallics*, 2006, **25**, 4695–4697.
29 H. W. Xu, P. G. Williard and W. H. Bernskoetter, *Organometallics*, 2012, **31**, 1588–1590.
30 W. J. Evans and D. K. Drummond, *Organometallics*, 1988, **7**, 797–802.
31 M. G. Gardiner, A. N. James, C. Jones and C. Schulten, *Dalton Trans.*, 2010, **39**, 6864–6870.
32 S. Hasegawa, Y. Ishida and H. Kawaguchi, *Chem. Commun.*, 2021, **57**, 8296–8299.
33 M. E. Garner, S. Hohloch, L. Maron and J. Arnold, *Angew. Chem., Int. Ed.*, 2016, **55**, 13789–13792.
34 I. J. Casely, J. W. Ziller and W. J. Evans, *Organometallics*, 2011, **30**, 4873–4881.
35 B. J. Deelman, W. M. Stevels, J. H. Teuben, M. T. Lakin and A. L. Spek, *Organometallics*, 1994, **13**, 3881–3891.
36 K. H. Denhaan, Y. Wielstra and J. H. Teuben, *Organometallics*, 1987, **6**, 2053–2060.
37 R. Duchateau, E. A. C. Brussee, A. Meetsma and J. H. Teuben, *Organometallics*, 1997, **16**, 5506–5516.
38 A. V. Karpov, A. S. Shavyrin, A. V. Cherkasov, G. K. Fukin and A. A. Trifonov, *Organometallics*, 2012, **31**, 5349–5357.
39 D. Robert, P. Voth, T. P. Spaniol and J. Okuda, *Eur. J. Inorg. Chem.*, 2008, 2810–2819.
40 J. Sun, D. J. Berg and B. Twamley, *Organometallics*, 2008, **27**, 683–690.
41 P. S. Coan, L. G. Hubertpfalzgraf and K. G. Caulton, *Inorg. Chem.*, 1992, **31**, 1262–1267.
42 W. J. Evans, J. H. Meadows, A. G. Kostka and G. L. Closs, *Organometallics*, 1985, **4**, 324–326.
43 G. Ballmann, H. Elsen and S. Harder, *Angew. Chem., Int. Ed.*, 2019, **58**, 15736–15741.
44 A. G. Coutsolelos, A. Tsapara, D. Daphnomili and D. L. Ward, *J. Chem. Soc., Dalton Trans.*, 1991, 3413–3417.
45 Y. Bouzidi, L. Belkhiri, M. Ephritikhine, J. F. Halet and A. Boucekkine, *J. Organomet. Chem.*, 2017, **847**, 82–89.
46 X. T. Chen, Q. N. Li, Y. Gong, L. Andrews, B. K. Liebov, Z. T. Fang and D. A. Dixon, *Inorg. Chem.*, 2017, **56**, 5060–5068.
47 A. Herve, Y. Bouzidi, J. C. Berthet, L. Belkhiri, P. Thuery, A. Boucekkine and M. Ephritikhine, *Inorg. Chem.*, 2015, **54**, 2474–2490.
48 J. C. Berthet, P. Thuery and M. Ephritikhine, *Dalton Trans.*, 2015, **44**, 7727–7742.
49 A. Herve, Y. Bouzidi, J. C. Berthet, L. Belkhiri, P. Thuery, A. Boucekkine and M. Ephritikhine, *Inorg. Chem.*, 2014, **53**, 6995–7013.
50 D. Lauvergnat, P. Maitre, P. C. Hiberty and F. Volatron, *J. Phys. Chem.*, 1996, **100**, 6463–6468.
51 H. A. Bent, *Chem. Rev.*, 1961, **61**, 275–311.
52 F. Weinhold and C. R. Landis, *Valency and Bonding: A Natural Bond Orbital Donor-Acceptor Perspective*, Cambridge University Press, Cambridge, 2005.
53 A. L. Odom, in *Comprehensive Organometallic Chemistry IV*, ed. P. Holland, Elsevier, 2022, vol. 1, pp. 2–30.
54 P. K. Hurlburt, J. J. Rack, J. S. Luck, S. F. Dec, J. D. Webb, O. P. Anderson and S. H. Strauss, *J. Am. Chem. Soc.*, 1994, **116**, 10003–10014.
55 A. J. Lupinetti, S. H. Strauss and G. Frenking, in *Prog. Inorg. Chem.*, ed. K. D. Karlin, 2001, vol. 49, pp. 1–112.
56 S. H. Strauss, *J. Chem. Soc., Dalton Trans.*, 2000, 1–6.
57 M. Finze, E. Bernhardt, H. Willner and C. W. Lehmann, *J. Am. Chem. Soc.*, 2005, **127**, 10712–10722.
58 V. S. Rao, A. Vijay and A. K. Chandra, *Can. J. Chem.*, 1996, **74**, 1072–1077.
59 M. H. Baghal-Vayjooee, J. L. Collister and H. O. Pritchard, *Can. J. Chem.*, 1977, **55**, 2634–2636.
60 M. R. Booth and S. G. Frankiss, *Spectrochim. Acta, Part A*, 1970, **26**, 859.
61 M. R. Booth and S. G. Frankiss, *Chem. Commun.*, 1968, 1347.
62 Here, we are using the ionic bond order divided by the total bond order from the NRT times 100 to give % ionic for the bond.
63 T. Stuyver and S. Shaik, *J. Am. Chem. Soc.*, 2020, **142**, 20002–20013.
64 J. S. M. Anderson, J. Melin and P. W. Ayers, *J. Mol. Model.*, 2016, **22**, 1–11.
65 J. S. M. Anderson, J. Melin and P. W. Ayers, *J. Chem. Theor. Comput.*, 2007, **3**, 358–374.
66 J. S. M. Anderson, J. Melin and P. W. Ayers, *J. Chem. Theor. Comput.*, 2007, **3**, 375–389.